PHYSICAL REVIEW D **74,** 123515 (2006)

X-ray radiation from the annihilation of dark matter at the galactic center

Lars Bergström[*] and Malcolm Fairbairn[†]

Cosmology, Particle Astrophysics and String Theory, Department of Physics, Stockholm University, AlbaNova University Centre, SE-106 91, Stockholm, Sweden

Lidia Pieri[‡]

INAF—Astronomical Observatory of Padova, Vicolo dell'Osservatorio 5, I - 35122 Padova, Italy and INFN—Sezione di Padova

(Received 14 August 2006; published 21 December 2006)

The existing and upcoming multiwavelength data from the galactic center suggest a comparative study in order to propose or rule out possible models which would explain the observations. In this paper we consider the x-ray synchrotron and the gamma-ray emission due to Kaluza-Klein dark matter and define a set of parameters for the shape of the dark matter halo which is consistent with the observations. We show that for this class of models the existing Chandra x-ray data are more restrictive than the constraints on very high energy gamma rays coming from HESS.

DOI: 10.1103/PhysRevD.74.123515 PACS numbers: 95.35.+d, 11.10.Kk, 98.35.Jk, 98.70.Qy

I. INTRODUCTION

Combined data from the cosmic microwave background (CMB) radiation, the distant type 1a supernovae, and the large scale structure studies suggest that approximately 25% of the density content of the Universe is nonbaryonic dark matter (dark matter) [1]. Weakly interacting massive particles (WIMPs), such as stable neutralinos in supersymmetric (SUSY) extensions of the standard model [2] or Kaluza-Klein (KK) particles in theories where there is a TeV^{-1} size universal extra dimension into which all standard model fields propagate [3,4], are exciting candidates since they can freeze out leaving a similar relic abundance to what is observed.

Neutralino or KK particle annihilation into standard model particles may be detected astrophysically [5] by observations of the regions of the Universe where the dark matter is expected to be densest. *N*-body simulations suggest that dark matter halos may have cuspy density profiles with large density peaks in the core. It is thought that the center of the Milky Way might contain such a dark matter overdensity, but it is also clear from observations that the gravitational field in the very central region is dominated by the $2.87 \pm 0.15 \times 10^6 M_\odot$ supermassive black hole [6] which resides there. The products of any dark matter annihilations will therefore be injected into the plasma falling into the central black hole. In this work we calculate the signal expected from the synchrotron radiation due to the annihilation of KK particles into electrons and positrons near the galactic center (GC).

Dark matter annihilation products depend upon the type of candidate involved. For instance, direct annihilation of SUSY dark matter into light fermions is highly suppressed and only low energy secondary electrons and positrons can arise as annihilation products. In KK scenarios there are universal extra dimensions with TeV^{-1} size into which the standard model fields propagate and there is an orbifold condition which renders the lightest KK mode stable [4]. In this model, the lightest KK mode is well approximated by the first KK mode of the B component of the electroweak field and therefore couples to standard model fermions and not gauge bosons (although photons may be produced via bremsstrahlung processes [7]). The annihilation into light fermions is no longer helicity suppressed and one might expect hard electrons from direct annihilation.

Since the electrons produced in the annihilation of SUSY dark matter typically have rather low energies compared to those produced in KK dark matter annihilation, their synchrotron radiation has a correspondingly smaller frequency. Synchrotrons from the electrons arising from the annihilation of SUSY WIMPs (studied in detail in Ref. [8]) would emerge at a frequency where there is either a lot of emission from the infalling gas, or in a frequency band where one would expect a large amount of extinction. In contrast, synchrotrons from the hard electrons produced by the annihilation of KK particles will emerge at much higher frequencies and peaks close to the region of sensitivity of the Chandra x-ray telescope, which conveniently has extremely good angular resolution. The background emission from Sagittarius A* is also lower in this region of frequency space, increasing the possibility of detection of a signal from the dark matter. We will therefore concentrate on these hard electrons from KK WIMP annihilation, rather than the electrons from SUSY WIMP annihilation (we refer the reader to Ref. [8] for a detailed analysis of the latter).

[*]Electronic address: lbe@physto.se
[†]Electronic address: malc@physto.se
[‡]Electronic address: lidia.pieri@oapd.inaf.it

II. GALACTIC CENTER

Multiwavelength observations of the galactic center, which we review in Fig. 1 [9], have led to various models to explain the observed emission from the central black hole. The consensus at the time of writing is that the sub-Eddington accretion flow onto the black hole is fueled by stellar mass loss from the cluster of large mass stars which exists in that region [10–12]. The radio, mm, and infrared radiation is thought to come from the inner regions of this flow close to the black hole, whereas the x-ray emission observed by Chandra is thought to originate further from the black hole, close to the Bondi radius at the interface between the spherical inflow region and the stellar winds where the gravity of the black hole starts to dominate the dynamics of the gas [13,14]. The Bondi radius is thought to be at around 0.04 pc from the central black hole, rather close to the 1 arcsecond resolution of the Chandra telescope at this distance. HESS observations [15] which have recently been confirmed by the MAGIC experiment [16] show that there is significant TeV gamma-ray emission from the central 30 pc around the black hole. This emission might be due to a number of things: it may come from annihilation of dark matter [7,17–19] or Fermi acceleration in the shock fronts of stellar winds [20], it may be a product of the interaction of ultra high energy protons with the ambient photons and magnetic field, it may come from proton-proton interactions in the accretion disk, or it may be generated by curvature and inverse Compton emission of accelerated electrons close to the black hole [21]. Recently it has been pointed out that this emission may hinder searches for the annihilation of dark matter because it provides too great a background [22].

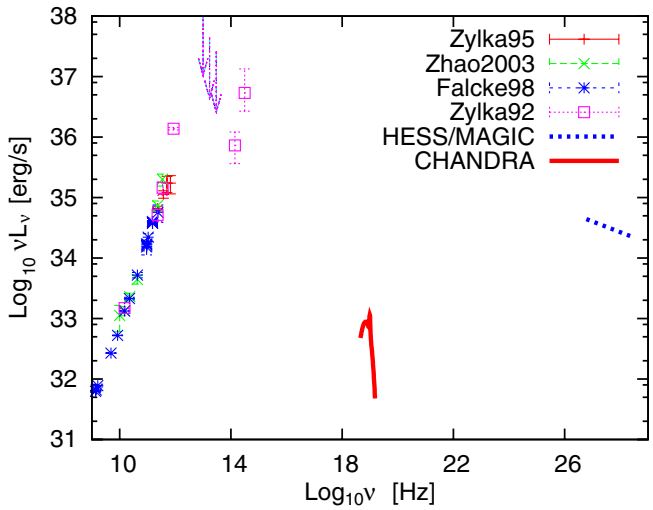

FIG. 1 (color online). Multiwavelength luminosity of Sgr A* in the quiescent state. Observations in the radio and infrared radiation come from Refs. [37–40]. The Chandra data are reconstructed from Ref. [13]. The HESS/MAGIC spectrum is plotted as one line since the two experiments are in agreement with each other [15,16].

In order to calculate the expected luminosity coming from the annihilation of WIMPs, one first needs to know what the density profile is within the region in question. Many N-body simulations predict that the density at the center of dark matter halos will asymptote to a power law $\rho \propto r^{-\gamma}$ [23–25], so the simplest approach is to assume a simple power law and to normalize it so that the local density at the sun is 0.3 GeV cm^{-3}. Assuming the emission along the line of sight is dominated by the galactic central region, the luminosity expected from that region is given by

$$L = f_{\rm em}\langle\sigma_{\rm tot}v\rangle m_{\rm dm} 4\pi \int_{r_{\rm min}}^{r_{\rm max}} \left(\frac{\rho(r)}{m_{\rm dm}}\right)^2 r^2 dr, \qquad (1)$$

where $f_{\rm em} \sim 0.5$ is the fraction of all the final states like electrons, muons, taus, and quark jets that will give rise to electromagnetic energy and $\langle\sigma_{\rm tot}v\rangle$ is the total thermally averaged KK particle annihilation cross section. The inner radius $r_{\rm min}$ is the cutoff radius below which there is a maximum density core due to the high self-annihilation rate. If we assume that the dark matter halo has existed for a time τ_h then the radius $r_{\rm min}$ is defined by $\rho(r_{\rm min}) = m_{\rm dm}\langle\sigma_{\rm tot}v\rangle/\tau_h$. The outer radius $r_{\rm max}$ corresponds to the angular resolution of the instrument in question at the distance corresponding to the center of the Galaxy. This

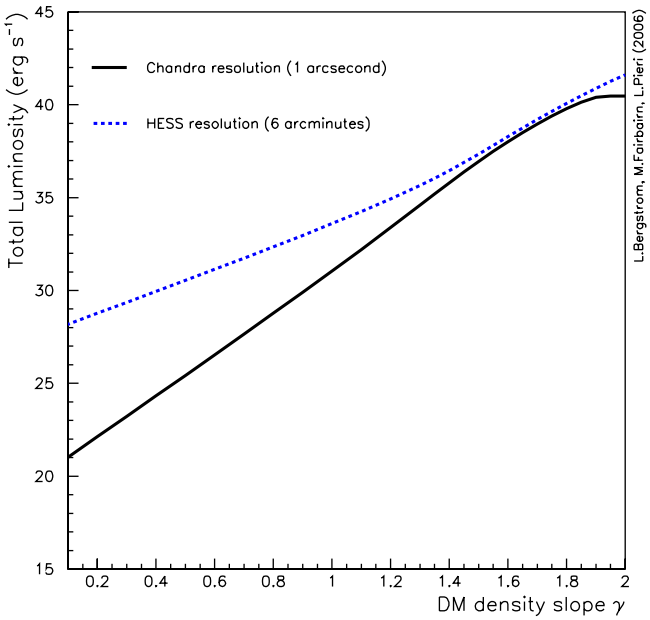

FIG. 2 (color online). Expected total luminosity from the center of the Galaxy for different dark matter profiles of the form $\rho \propto r^{-\gamma}$ normalized to 0.3 GeV cm^{-3} at the sun, for $\langle\sigma_{\rm tot}v\rangle = 3 \times 10^{-26}$ cm^3 s^{-1} and $m_{\rm dm} = 1$ TeV. Since the emission is diffuse, the two curves correspond to 6 arcminutes (HESS) and arcsecond (Chandra) angular resolution. We assume a maximum density in the core due to self-annihilation (see text). The luminosity stops growing for the Chandra case when the entire region within the Chandra angular resolution is at the maximum density of dark matter.

may be an underestimate since the contribution from the dark matter at $r > r_{\rm max}$ along the line of sight is not considered. However, in our models, which have rather steep central densities, the assumption that the dark matter emission emanates entirely from a sphere with radius corresponding to the angular resolution of the instrument is a good approximation. Equation (1) can therefore be considered a correct estimate. In Fig. 2 we give the luminosity expected to lie within the beam of an arcminute resolution device such as HESS or GLAST and an arcsecond resolution telescope such as Chandra.

Typical values of the asymptotic power law for the density profile in the inner regions found in N-body simulations are $\gamma \sim 1$–1.5. The quiescent x-ray emission observed by Chandra is around 10^{33} erg s^{-1}, which is interesting as it is rather close to the emission that one would expect from the annihilation of WIMPs from the same region for these values of γ.

Generation of energetic electrons in a magnetized plasma will lead to synchrotron radiation and, in order to predict the synchrotron spectrum, we need a model for the magnetic field around the center of the Galaxy.

III. MAGNETIC FIELD

Radio observations of the galactic center show some evidence of variability thought to be associated with a very small central accretion disk at a scale of 2.7×10^{-4} arcseconds, i.e. 40 $R_{\rm BH}$ [26], where $R_{\rm BH} \sim 7 \times 10^{11}$ cm is the Schwarzschild radius for the black hole. At much larger radii it is therefore valid to assume the behavior of the magnetic field is governed by the general theory of quasispherical infall. Observations over many years also show that, despite flaring, accretion onto Sagittarius A* appears to be quasistatic over time (see e.g. [27]).

The theory of quasistatic infalling plasma predicts a magnetic field profile of the form $B(r) \sim r^{-2}$. This power law holds until some radius $r_{\rm equi}$ at which equipartition between magnetic and kinetic energy is achieved,

$$\frac{\rho(r)v(r)^2}{2} = \frac{B^2(r)}{8\pi}. \tag{2}$$

For radii smaller than $r_{\rm equi}$, accretion is possible only if the magnetic field is destroyed and the magnetic energy dissipated. There are strong constraints on the approximate strength of the magnetic field in the central regions in order to agree with the observed sub-mm radiation [11,12].

The simplest way to normalize the strength of the magnetic field in the GC is to assume that the inflowing gas is due to the stellar outflow from large stars in the center of the Galaxy [10]. This gives rise to a mass inflow at the accretion radius, which sets the electron density and equipartition magnetic fields from that radius downwards.

In our model we have $r_{\rm equi} \sim 0.04$ pc and $\dot{M} = 10^{22}$ gs^{-1} and, if we assume standard spherical Bondi-Hoyle accretion below that radius, we then have an equipartition magnetic field of strength

$$B_{\rm eq}(r) = 3.9 \times 10^{-2} \left(\frac{0.01 \text{ pc}}{r}\right)^{5/4} \text{ Gauss} \tag{3}$$

in agreement with the authors of [8].

It has been pointed out, however, that the equipartition picture may not be correct at very small distances from the GC, where magnetic field line reconnection in the turbulent plasma may reduce the magnetic field. We will therefore also calculate the spectrum corresponding to the following modified magnetic field:

$$\begin{aligned} B_m(r) &= B_{\rm eq}(r), && r > 10^3 R_{\rm BH}, \\ B_m(r) &= B_{\rm eq}(10^3 R_{\rm BH}), && 3R_{\rm BH} < r < 10^3 R_{\rm BH}, \\ B_m(r) &= B_{\rm eq}(3R_{\rm BH}) \left(\frac{r}{3R_{\rm BH}}\right)^{-3}, && R_{\rm BH} < r < 3R_{\rm BH}. \end{aligned} \tag{4}$$

Here the various length scales have been taken from the reconnected field in Ref. [28], although the overall strength of that field is slightly lower at large radii than the naive equipartition value which we adopt. The two magnetic fields are plotted in Fig. 3. To a first approximation, it turns out that the synchrotron spectrum arising from the annihilation of dark matter in our region of interest ($\sim 10^{19} - 10^{20}$ Hz) is not particularly sensitive as to whether one

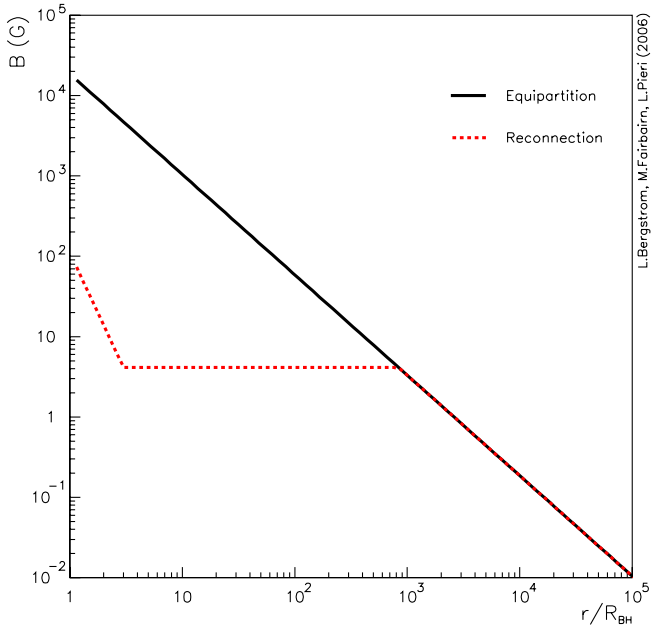

FIG. 3 (color online). Assumed magnetic field as a function of radius from the black hole. The solid line corresponds to the equipartition magnetic field of Eq. (3), whereas the red dashed line is the flux-reconnection magnetic field of Eq. (4).

chooses the B field described by Eq. (3) or (4), at least in the window of sensitivity of Chandra.

There is rather a lot of uncertainty in the values of the magnetic fields which should be adopted in this very central region of the Galaxy, but we will show that the spectra in the region of interest are not extremely sensitive to the magnetic field.

IV. ENERGY LOSS MECHANISMS

Since the synchrotron lifetime of TeV electrons in this environment is much shorter than the time scales of any of the other energy loss mechanisms, we can neglect them in the solution to the diffusion-loss equation. For example, at these high energies, radiative processes dominate and energy losses for an electron with energy E via a radiative mechanism X can be expressed in the form

$$\dot{E} = \tfrac{4}{3} c \sigma_T U_X \gamma^2, \tag{5}$$

where γ is the Lorentz factor and U_X represents the energy density contained in the magnetic field for synchrotron losses, the background radiation field for inverse Compton scattering (ICS) or the synchrotron radiation itself for synchrotron self-Comptonization (SSC). If we consider ICS then the CMB will contribute 0.25 eV cm^{-3}, whereas normal stellar radiation will contribute a few eV cm^{-3} [8]. With the fields that we have assumed, the magnetic field $B > 10^{-2}$ G in the region of interest which corresponds to $U_{\rm sync} \propto B^2 \geq 10^6$ eV cm^{-3}, much larger than $U_{\rm ICS}$ in the central accretion region. While subdominant, the ICS radiation will emerge at much higher energies than x-ray radiation; for example, the CMB photons will be scattered to tens of MeV, the region soon to be probed by the GLAST mission.

One can show that the SSC is subdominant through numerical integration over the synchrotron flux to obtain $U_{\rm SSC}$. A simpler, rougher way of seeing this is by checking that the (over-)estimate of $U_{\rm SSC}$ obeys the inequality

$$U_{\rm SSC} \simeq \frac{Lr}{4\pi r^3 c} \ll \frac{B^2}{8\pi} = U_{\rm sync}, \tag{6}$$

where L is the luminosity of the system, r is the radius, and c is the speed of light. This is simply the amount of synchrotron radiation that one would expect to flow through a unit volume at a given radius due to the total luminosity at smaller radii. Since the dark matter profiles we consider are rather steep, most of the emission will come from smaller radii rather than from larger radii which is why this is a good approximation to the full integral over all radii to obtain the background synchrotron photons.

In the results that we present below, it turns out that only for the reconnection magnetic field and the most spiked profiles [profile (C) below] could this inequality be in danger, and then only in a small region of the emission region close to the black hole. Since we will see that such profiles are already ruled out by gamma-ray observations, we conclude that we do not need to worry about synchrotron self-absorption at the level of accuracy of this paper.

Other time scales are also larger than the energy loss time scale. For example, the gravitational infall time scale compared with the synchrotron time scale for a TeV electron in the equipartition field (3) is given by

$$\begin{aligned} \tau_{\rm grav} &= \sqrt{\frac{r^3}{GM_{\rm BH}}} = 2.7 \times 10^8 \left(\frac{r}{0.01\ {\rm pc}}\right)^{3/2}\ {\rm sec}, \\ \tau_{\rm sync} &= \frac{3}{4\sigma_T c}\frac{8\pi}{B^2}\frac{E}{\gamma^2} = 2.6 \times 10^5 \left(\frac{r}{0.01\ {\rm pc}}\right)^{5/2}\ {\rm sec} \end{aligned} \tag{7}$$

so that $\tau_{\rm grav} \gg \tau_{\rm sync}$, demonstrating our point. The characteristic time scale upon which the synchrotron time scale itself varies is very close to the gravitational time scale.

We assume that the electrons lose energy before they change position significantly. In order for this to be true, the diffusion length scale should be much smaller than the radial distance of the electron from the central black hole. We obtain the diffusion length scale in the same way as the authors of Ref. [29] by taking the geometric average of the magnetic diffusion length scale d_B (taken to be one-third of the gyromagnetic radius) with the distance corresponding to the synchrotron lifetime $c\tau_{\rm sync}$.

$$\frac{\sqrt{c\tau_{\rm sync} d_B}}{r} = \frac{m_e}{r}\sqrt{\frac{2\pi}{e\sigma_T B^3}} = 2.78 \times 10^{-4}\left(\frac{r}{0.01\ {\rm pc}}\right)^{7/8} \tag{8}$$

so that the diffusion of the electrons can also be neglected.

We will therefore assume that all terms other than synchrotron energy loss can be set to zero, which would certainly not be true for electrons arising from SUSY WIMP annihilations.

When considering direct dark matter annihilation into electrons, we will be interested in a delta function of electrons with energy $m_{\rm dm}$. The solution of the diffusion-loss equation then has the following form:

$$\frac{dn}{dE}(E, r) = \frac{1}{2}\left(\frac{\rho(r)}{m_{\rm dm}}\right)^2 \langle \sigma_{\rm tot} v \rangle N_{ee} b_{ee} \frac{1}{\dot{E}}\ {\rm cm}^{-3}\,{\rm GeV}^{-1} \tag{9}$$

which is valid over a range of energies, $E < m_{\rm dm}$. $N_{ee} = 2$ is the overall number of electrons and positrons produced in each annihilation and $b_{ee} = 0.19$ is the branching ratio of annihilation in the electron-positron line. We used $\langle \sigma_{\rm tot} v \rangle = 3 \times 10^{-26}$ cm^3 s^{-1}. $N(E, r)$ is zero for $E > m_{\rm dm}$.

V. DARK MATTER DENSITY PROFILES

The dark matter density profile, $\rho(r)$, at the GC is a subject of rich debate. N-body simulations predict a den-

TABLE I. Parameters of the density profiles [see Eq. (10)]. These are approximations of the profiles presented in [34].

Profile	$\rho(100\ \mathrm{pc})$	γ_1	γ_2	r_{out}	r_{in}
(A)	25 GeV/cm^3	1	...	0	0
(B)	25 GeV/cm^3	1	1.85	$7 \times 10^4 R_{\mathrm{BH}}$	$10 R_{\mathrm{BH}}$
(C)	360 GeV/cm^3	1.5	1.82	$7 \times 10^4 R_{\mathrm{BH}}$	$10 R_{\mathrm{BH}}$

sity profile with an asymptotic power law behavior in the central region, the density rising as $\rho \propto r^{-\gamma}$ with different predictions for γ ranging between 1 and 1.5 [23–25]. Other predictions suggest that the value of γ changes steadily as one approaches the center of the halo [30].

At the same time, it is well known that baryons in gravitationally bound systems lose energy and fall to the center, creating an enhanced potential well into which the dark matter is then drawn [31]. This phenomenon of adiabatic contraction is not completely understood, especially in the very central regions of the Galaxy, although attempts to take into account the noncircularity of the orbits seem to help [32].

It has also been suggested that the profile of dark matter in the immediate vicinity of the GC is enhanced during the period of formation of the black hole [33]. This would lead to a rather dense "spike" of dark matter at the center which would in turn give rise to large annihilation rates. However, more recently it has been argued that the dark matter in this spike would be heated by the gravitational dynamical friction of the stellar population, leading somewhat to its dispersion [34]. We will use the results of the numerical work of Ref. [34] to obtain hopefully realistic models of the dark matter profile near the center of the Galaxy.

In light of the above discussion, we consider three density profiles for the dark matter distribution, all of which can be parametrized rather simply by the following expression:

$$\begin{aligned} \rho(r) &= \rho(100\ \mathrm{pc})\left(\frac{100\ \mathrm{pc}}{r}\right)^{\gamma_1}, \quad && r > r_{\mathrm{out}}, \\ \rho(r) &= \rho(r_{\mathrm{out}})\left(\frac{r_{\mathrm{out}}}{r}\right)^{\gamma_2}, \quad && r_{\mathrm{out}} > r > r_{\mathrm{in}}, \\ \rho(r) &= \rho(r_{\mathrm{in}}), && r_{\mathrm{in}} > r. \end{aligned} \tag{10}$$

The three models we will consider are (A) the standard Navarro, Frenk, and White (NFW) $\gamma = 1$ profile with no adiabatic contraction or central spike, (B) the same $\gamma = 1$ profile, but now with a central spike which has diffused away over time, considerably reducing its density, and (C) a profile which has undergone adiabatic contraction on galactic scales due to the presence of baryons, and also has a central spike that is allowed to diffuse away over time. The profiles are summarized in Table I and plotted in Fig. 4.

For profile (A) $r_{\mathrm{out}} = r_{\mathrm{in}} = 0$ and $\rho(100\ \mathrm{pc}) = 25\ \mathrm{GeV/cm^3}$, where the value of the density is obtained by normalizing to the canonical density 0.3 GeV/cm^3 at the solar radius. The parameters for profiles (B) and (C) are obtained by making approximate fits to the results published in Fig. 1 of Ref. [34]. For both profiles $r_{\mathrm{out}} = 7 \times 10^4 R_{\mathrm{BH}}$ and $r_{\mathrm{in}} = 10 R_{\mathrm{BH}}$.

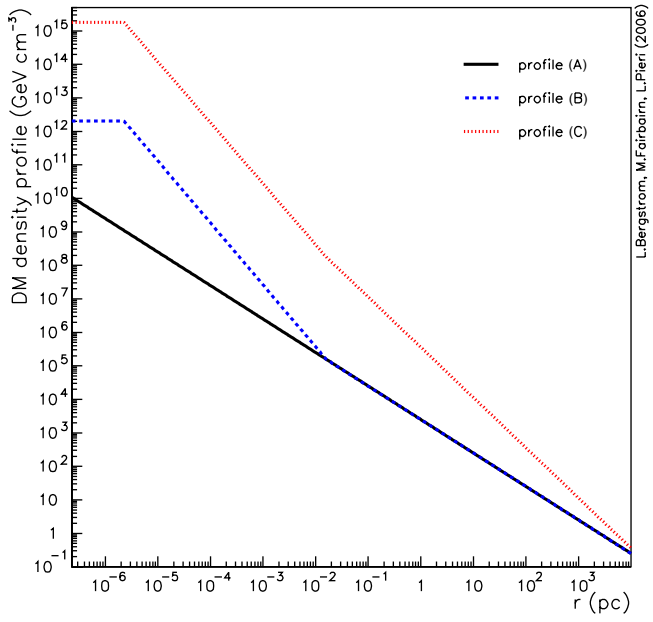

FIG. 4 (color online). Density profiles used in this work and presented in Table I.

VI. RESULTS

The x-ray synchrotron flux emitted in the central region of the Galaxy is attenuated mainly via photoelectric absorption, which is the dominant process for x-ray absorption up to energies of at least 100 keV. This effect depends weakly upon atomic arrangement and can be computed considering free atoms. The magnitude of the effect therefore depends upon the column density of electrons along the line of sight N_H, which we set equal to $1.5 \times 10^{23}\ \mathrm{cm}^{-2}$ [35], and on the photoelectric cross section $\sigma_{\mathrm{p.e.}}$ [36].

Because we ignore all energy loss effects other than synchrotrons, the equations for emissivity and luminosity simplify considerably. We define r_{res} to be the radius corresponding to the angular resolution of Chandra and $f(\nu', \nu)$ the fraction of synchrotron radiation emitted at a frequency ν' from an electron circling with a synchrotron frequency ν. The observed luminosity in synchrotron radiation of frequency ν' is then well approximated by the expression

$$\nu' L_{\nu'} = \frac{1}{2}\langle\sigma_{\rm tot} v\rangle N_{\rm ee} b_{\rm ee} m_e \int_0^{r_{\rm res}} 4\pi r^2 \left(\frac{\rho(r)}{m_{\rm dm}}\right)^2 \times \exp(-N_H \sigma_{\rm p.e.}(\nu')) \int_0^{\infty} f(\nu', \nu) \times \theta\left(1 - \frac{\nu_*}{B_*(r)}\frac{m_e}{m_{\rm dm}}\right)\sqrt{\frac{\nu_*}{B_*(r)}} d\nu dr, \quad (11)$$

where the dimensionless quantity ν_* is ν/Hz, $B_* = B/2.8 \times 10^{-6}$ G, and θ is the Heaviside step function. The function $f(\nu', \nu)$ is defined to be

$$f(\nu', \nu) = x \int_x^{\infty} K_{5/3}(y) dy, \qquad x = \frac{\nu'}{\nu}, \quad (12)$$

where $K_{5/3}$ is a modified Bessel function.

Figure 5 shows the synchrotron spectra from a 1 TeV KK particle annihilation in the GC, for the different density profiles described in Eq. (8) and for the different magnetic field assumption of Eqs. (3) and (4).

In order to find out if the x-ray emission predicted in our model is reasonable, we have to compare it with the HESS data to make sure that the halos we consider do not give rise to too much emission in gamma rays. First we assume that the HESS resolution corresponds to a 30 pc radius sphere around the GC [15]; then we note that the authors of [7] fit the HESS data with an NFW $\gamma = 1$ profile and a boost factor of 200 in the flux. It is therefore necessary to ensure that the profiles that we use are not so dense as to saturate this bound; otherwise one would expect more emission in the form of TeV gamma rays than observed by HESS. The HESS bound corresponds to a total luminosity from within the 30 pc sphere of about 6.9×10^{37} GeV s^{-1}, whereas the three profiles, (A), (B), and (C), that we have considered correspond to 3.5×10^{30}, 5.5×10^{35}, and 1.3×10^{41} GeV s^{-1}, respectively, so that profile (C) is ruled out.

Profile (B), which does not violate the bound from HESS, gives rise to approximately the same flux as the observed signal from Chandra in the region of interest, as can be seen in Fig. 6. In this way one can claim that x-ray observations are therefore more restrictive than TeV observations, since they rule out density profiles which are less steep than those ruled out by HESS.

It would be tempting to argue that the observed emission in x rays could be explained via dark matter synchrotrons rather than thermal bremsstrahlung. As we see in Fig. 2, the flux from dark matter synchrotrons is certainly conceivably of the right order of magnitude, although the spectrum seems to have the wrong shape given the magnetic fields

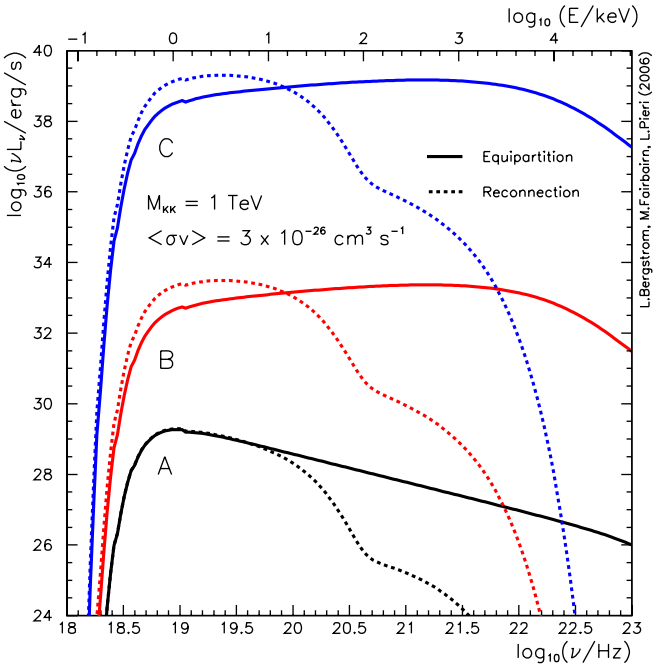

FIG. 5 (color online). Synchrotron spectra from 1 TeV KK dark matter annihilation in the central 0.01 pc of the Galaxy assuming the three density profiles—(A), (B), (C)—described in Eq. (10). The solid lines correspond to the equipartition magnetic field of Eq. (3) and the dotted lines are the spectra with the flux-reconnection magnetic field of Eq. (4).

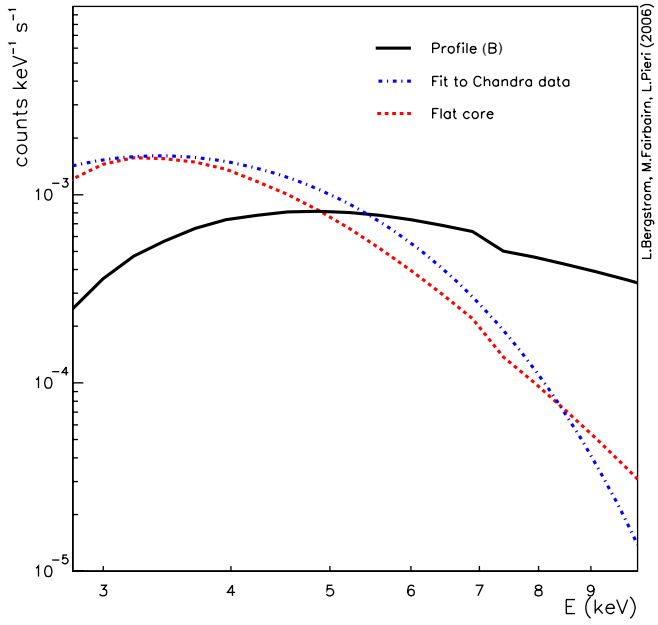

FIG. 6 (color online). Comparison of profile (B) with Chandra data: the dot-dashed curve is an approximate fit to the data presented in [14] without the iron line. The solid curve is the signal expected from synchrotron radiation from electrons produced in dark matter annihilations assuming density profile (B). The dashed curve corresponds to the synchrotron radiation from the flat core described in the text. We assume a Chandra effective aperture of 400 cm^2.

considered in this work. There is also the observation of an iron line [13], a spectral feature which could not be explained very easily by synchrotrons.

It would be interesting to see if it is possible to fit the continuum emission observed by Chandra and assumed to be thermal bremsstrahlung. The observed spectrum drops more rapidly than our synchrotron, so we need to assume a magnetic field of the form (4) but with a strength 1 order of magnitude smaller than that plotted in Fig. 3, so that its maximum is at a lower energy than the absorption cutoff at 2 keV. If we then assume a core of dark matter with constant density of around $10^8 M_\odot$ pc^{-3}, then we can obtain a spectrum rather close to what is observed.

While this is an amusing result, it would be rather optimistic to claim that the continuum component of x rays observed at the galactic center comes from the synchrotron radiation associated with dark matter electrons. Nevertheless, we feel it is important to note that the energy injected into the plasma in the form of electrons is significant compared to the energy emitted in the x-ray region of the spectrum. A more detailed study of the effect of these electrons as they thermalize and heat the local environment might be worthwhile.

To be consistent with the studies [7,17,19], we can also consider the spectra emitted for different masses of the KK particle. This is perhaps not so interesting for the case of universal extra dimensions, because it is only when the KK particle has a mass close to 1 TeV that one obtains a good relic abundance. However, for the sake of completeness we have calculated the spectra for a 10 TeV particle which annihilates into electrons with the same branching ratio as KK particles in Fig. 7.

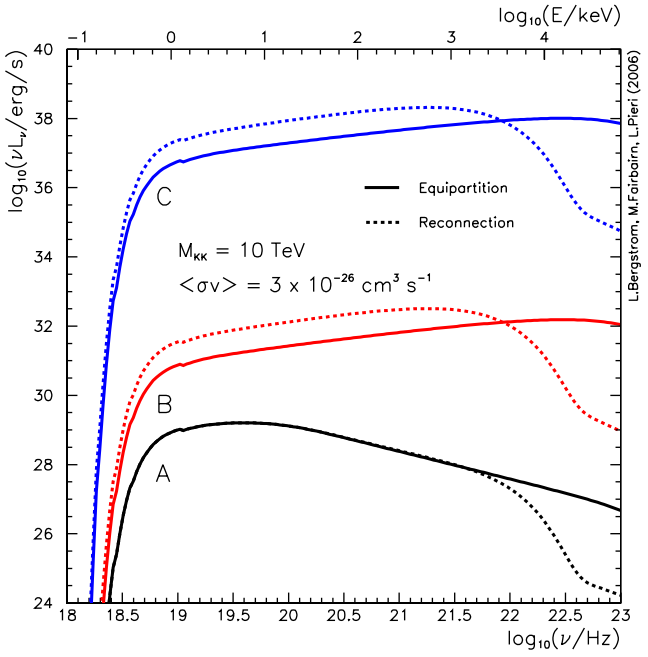

FIG. 7 (color online). Synchrotron spectra from 10 TeV KK dark matter annihilation in the central 0.01 pc of the Galaxy assuming the three density profiles—(A), (B), (C)—described in Eq. (10). The solid lines correspond to the equipartition magnetic field of Eq. (3) and the dotted lines are the spectra with the flux-reconnection magnetic field of Eq. (4).

We have therefore presented the expected spectra from dark matter for three density profiles which seem to be well motivated from astrophysical considerations at the time of writing. A more general approach to the density profiles, which may be more appropriate given the large amount of uncertainties involved in their derivation, is the following. We assume that the density of dark matter at the solar radius is 0.3 GeV cm^{-3} and then we choose a single power law that is valid down to very small radii. This is clearly unrealistic at the very center of the Galaxy due to the dynamics discussed in the previous section, but it does serve as a useful parametrization.

We find that the steepest profile which is compatible with the x-ray data is $r^{-1.35}$. The gamma rays produced by such a profile within the angular resolution of the HESS telescope array are much less than what is observed. Consequently, we find that the x-ray observations from Chandra can be much more restrictive than the data from gamma-ray telescopes with much larger angular uncertainties.

VII. CONCLUSIONS

In this paper we have calculated the expected x-ray synchrotron spectra flux from high energy electrons produced by the annihilation of KK dark matter particles at the galactic center. Many of our conclusions will be approximately valid for other TeV dark matter candidates which decay into hard fermions without helicity suppression.

We presented spectra for two different magnetic fields—one corresponding to equipartition with the plasma falling into the central black hole, and the other taking into account the possibility of flux reconnection which may occur due to turbulence in the infalling gas. We also looked at three different density profiles, showing how they affected the expected spectra.

The luminosity expected from the galactic center region due to the annihilation of WIMPs is rather close to what is actually observed (within a few orders of magnitude either way, depending upon the assumed density profile.) This is remarkable because the physics which governs the flux from dark matter annihilations is completely different from that governing the accretion onto the central black hole. The electrons injected into the plasma due to the annihilation of dark matter may therefore have a considerable effect upon the astrophysics of the central region around the black hole.

We found that the x-ray emission from the GC is not inconsistent with the annihilation of KK particles of mass 1 TeV, provided that the shape of the inner density profile is less steep than $r^{-1.35}$. Since the total luminosity corre-

sponding to this profile within the angular resolution of the HESS telescope is less than the luminosity which has been observed by HESS, we are able to claim that x-ray observations from Chandra are more constrictive than existing gamma-ray data. Because of this, it should be impossible to detect KK dark matter using gamma rays, since, if it were possible, the x-ray synchrotron signal of that dark matter should already have produced much more flux in x rays than what is observed in the Chandra data.

ACKNOWLEDGMENTS

L. B., M. F., and L. P. are grateful for receiving funding from the Swedish Research Council (Vetenskapsrådet).

[1] D. N. Spergel *et al.*, Astrophys. J. Suppl. Ser. **148**, 175 (2003).
[2] G. Jungman *et al.*, Phys. Rep. **267**, 195 (1996); G. Bertone, D. Hoooper, and J. Silk, Phys. Rep. **405**, 279 (2005).
[3] T. Appelquist *et al.*, Phys. Rev. D **64**, 035002 (2001).
[4] G. Servant and T. M. P. Tait, Nucl. Phys. **B650**, 391 (2003).
[5] L. Bergström, Rep. Prog. Phys. **63**, 793 (2000).
[6] R. Schoedel *et al.*, Astrophys. J. **596**, 1015 (2003).
[7] L. Bergström, T. Bringmann, M. Eriksson, and M. Gustafsson, Phys. Rev. Lett. **94**, 131301 (2005).
[8] R. Aloisio, P. Blasi, and A. V. Olinto, J. Cosmol. Astropart. Phys. 05 (2004) 007.
[9] The Chandra data were reconstructed assuming an effective area, defined as the product of the detection efficiency times the geometrical area of the detector of 400 cm^2.
[10] F. Melia, Astrophys. J. **387**, L27 (2003).
[11] S. Liu and F. Melia, Astrophys. J. **561**, L77 (2001).
[12] F. Yuan, E. Quataert, and R. Narayan, Astrophys. J. **598**, 301 (2003).
[13] Y. D. Xu, R. Narayan, E. Quataert, F. Yuan, and F. K. Baganoff, Astrophys. J. **640**, 319 (2006).
[14] F. K. Baganoff *et al.*, Astrophys. J. **591**, 891 (2003).
[15] F. Aharonian *et al.* (HESS Collaboration), Astron. Astrophys. **425**, L13 (2004).
[16] J. Albert *et al.* (MAGIC Collaboration), Astrophys. J. **638**, L101 (2006).
[17] D. Horns, Phys. Lett. B **607**, 225 (2005); **611**, 297(E) (2005).
[18] N. Fornengo *et al.*, Phys. Rev. D **70**, 103529 (2004).
[19] S. Profumo, Phys. Rev. D **72**, 103521 (2005).
[20] E. Quataert and A. Loeb, Astrophys. J. **635**, L45 (2005).
[21] F. Aharonian and A. Neronov, Astrophys. J. **619**, 306 (2005).
[22] G. Zaharijas and D. Hooper, Phys. Rev. D **73**, 103501 (2006).
[23] B. Moore, F. Governato, T. Quinn, J. Stadel, and G. Lake, Astrophys. J. **499**, L5 (1998).
[24] J. F. Navarro, C. S. Frenk, and S. D. M. White, Astrophys. J. **462**, 563 (1996).
[25] J. Diemand, M. Zemp, B. Moore, J. Stadel, and M. Carollo, Mon. Not. R. Astron. Soc. **364**, 665 (2005).
[26] S. S. Doeleman *et al.*, astro-ph/0102232.
[27] R. M. Herrnstein, J. H. Zhao, G. C. Bower, and W. M. Goss, astro-ph/0402543.
[28] R. F. Coker and F. Melia, Astrophys. J. **534**, 723 (2000).
[29] G. Bertone, G. Sigl, and J. Silk, Mon. Not. R. Astron. Soc. **326**, 799 (2001).
[30] J. F. Navarro *et al.*, Mon. Not. R. Astron. Soc. **349**, 1039 (2004).
[31] G. R. Blumenthal, S. M. Faber, R. Flores, and J. R. Primack, Astrophys. J. **301**, 27 (1986).
[32] O. Y. Gnedin, A. V. Kravtsov, A. A. Klypin, and D. Nagai, Astrophys. J. **616**, 16 (2004).
[33] P. Gondolo and J. Silk, Phys. Rev. Lett. **83**, 1719 (1999).
[34] G. Bertone and D. Merritt, Phys. Rev. D **72**, 103502 (2005).
[35] D. Porquet *et al.*, Astron. Astrophys. **407**, L17 (2003).
[36] Tabulated by G. Matt (private communication).
[37] R. Zylka *et al.*, Astron. Astrophys. **297**, 83 (1995).
[38] H. Falcke, W. M. Goss, H. Matsuo, P. Teuben, J. H. Zhao, and R. Zylka, astro-ph/9801085.
[39] J. H. Zhao *et al.*, Astrophys. J. **586**, L29 (2003).
[40] R. Zylka, P. Mezger, and H. Lesch, Astron. Astrophys. **261**, 119 (1992).